



Universiteit
Leiden
The Netherlands

Modulation of the Extracellular Matrix in Advanced Atherosclerosis

Nooijer, Ramon de

Citation

Nooijer, R. de. (2005, December 12). *Modulation of the Extracellular Matrix in Advanced Atherosclerosis*. Retrieved from <https://hdl.handle.net/1887/3751>

Version: Corrected Publisher's Version

License: [Licence agreement concerning inclusion of doctoral thesis in the Institutional Repository of the University of Leiden](#)

Downloaded from: <https://hdl.handle.net/1887/3751>

Note: To cite this publication please use the final published version (if applicable).

6

Leukocyte Cathepsin S Deficiency Decreases Atherosclerotic Plaque Collagen Content and Attenuates Macrophage Apoptosis

R. de Nooijer^{1,2}, J.H. von der Thüsen^{1,3}, M.A. Leeuwenburgh⁴, H.S. Overkleef⁴, R. Dorland¹, J.W. Jukema², E.E. van der Wall², Th.J.C. van Berkel¹, G.P. Shi⁵, E.A.L. Biessen¹

¹ Div. of Biopharmaceutics, Leiden University, 2333CC, Leiden, Netherlands

² Dept. of Cardiology, Leiden University Medical Centre, 2333ZA, Leiden, Netherlands

³ Dept. of Pathology, Leiden University Medical Centre, 2333ZA, Leiden, Netherlands

⁴ Div. of Bio-organic Synthesis, Leiden University, 2333CC, Leiden, Netherlands

⁵ Dept. of Medicine, Brigham and Women's Hospital and Harvard Medical School, Boston, Massachusetts, USA

Submitted

Abstract

A dysbalance of proteases and their inhibitors is instrumental in the remodeling of advanced plaques towards a more vulnerable phenotype. One of the proteases thought to be implicated in matrix degradation is cathepsin-S (CatS). To address its role in advanced lesions, we generated chimeric LDLr^{-/-} mice deficient in leukocyte CatS by transplantation with CatS^{-/-}xLDLr^{-/-} (n=11) or with LDLr^{-/-} bone marrow (n=11) and put them on a high-fat diet for 12 weeks. The aortic root was analyzed histologically.

No difference in lesion size could be detected between CatS^{+/+} and CatS^{-/-} chimeras. However, leukocyte CatS deficiency markedly changed plaque morphology and led to a dramatic reduction in necrotic core area (77%, P=0.001) and an abundance of large foam cells (P=0.006). Plaques of CatS^{-/-} chimeras contained 17% more macrophages (P=0.02), 62% less SMCs (P<0.001) and 33% less intimal collagen (p=0.02). The latter two could be explained by a reduced number of elastic lamina ruptures (68%, P=0.02). Moreover, macrophage apoptosis was reduced by 60% with CatS deficiency (P=0.001). In vitro, CatS inhibition did not affect spontaneous or oxLDL induced cell death. However, CatS was found to be involved in disruption of macrophages from a fibronectin or collagen matrix, and its inhibition could prevent apoptosis (P=0.06 and P<0.001).

In conclusion, CatS expression within the advanced plaque is of major importance not only for its matriceal, but also its cellular composition. Leukocyte CatS deficiency results in dramatically altered plaque morphology, with less necrotic cores, due to reduced apoptosis, and decreased SMC content and collagen deposition, as a result of impaired elastic lamina degradation.

Introduction

Proteolysis is an important process in the pathogenesis of atherosclerosis and thrombosis. Leukocyte transmigration through the endothelial basal membrane, smooth muscle cell (SMC) migration through the elastic lamina, and intimal neoangiogenesis all rely on degradation of the pericellular (PCM) and extracellular matrix (ECM).¹⁻³ Proteolytic enzymes like matrix metalloproteinases (MMPs) and cathepsins have been linked to ECM remodeling leading to arterial enlargement, formation of aneurysms and plaque disruption.⁴⁻⁷ Moreover, by releasing matrix-bound cytokines, chemokines and growth factors, proteases actively participate in cell recruitment, proliferation, apoptosis and inflammation.^{2, 8}

Cathepsins are enzymes with strong elastolytic and collagenolytic properties and form a distinct subgroup of atherosclerosis-related proteases because their physiological actions not only affect PCM/ECM degradation, but also directly modulate inflammation, immunogenic responses and cellular metabolism and turnover.⁹⁻¹² In fact, Cathepsin B (CatB) has been shown to activate IL-1 converting enzyme (ICE, caspase-1)¹³ and Cathepsin S (CatS) processes the invariant chain (Ii), a chaperone for major histocompatibility complex II (MHCII) and MHCI, therewith affecting antigen presentation and NK1.1(+) T-cell maturation.¹⁴⁻¹⁶ Furthermore, CatS inhibits HDL3 induced cholesterol efflux from macrophage foam cells and various cathepsins (e.g. D,F,S,K) are able to modify apoB100, cholesterol esters and triglycerides in LDL, inducing foam cell formation.¹⁷⁻¹⁹ CatS expression is stimulated by the pro-inflammatory cytokines IL-1 β , IFN- γ and TNF- α ²⁰, all of which have been linked to atherosclerosis.^{21, 22}

Recently Sukhova et al. proposed the involvement of CatS and CatK in atherogenesis, because CatS can be expressed by all atheroma associated cells, like endothelial cells, macrophages and smooth muscle cells (SMCs) and both its expression and activity are stimulated by a range of pro-inflammatory cytokines that are highly expressed in atherosclerotic plaques.^{20, 23-25} Also, CatS expression by macrophages at the shoulder regions was found to be increased, suggesting that this enzyme is involved in plaque rupture.²⁰ CatS deficiency attenuates plaque growth in LDLr knockout mice²⁶ and impairs intimal neovascularization²⁷, a process that is thought to be of major importance in atherosclerotic plaque progression and stability.²⁸

As CatS can exert a wide spectrum of physiological actions depending on its context, source, abundance and site of action it is important to dissect the cell specific functions of this enzyme in order to fully understand its role in atherogenesis. With the present study we aimed to define the leukocyte specific function of CatS. Chimeric LDLr^{-/-} mice deficient in leukocyte CatS were generated by bone marrow transplantation (BMT) of LDLr^{-/-} x CatS^{-/-} mice to irradiated LDLr^{-/-} mice. We found that leukocyte CatS deficiency leads to a markedly altered plaque morphology and composition, which could in part be attributed to fewer elastic lamina ruptures and a higher resistance to apoptosis and necrosis.

Materials and Methods

Animals and Study protocol

Female LDLr deficient mice (n=22), 20-24 weeks of age, were obtained from our own breeding stock (Gorlaeus Laboratories, Leiden, Netherlands) and irradiated with a lethal X-ray dose of 9 Gy as previously described.²⁹ Twenty-four hours after irradiation, mice were injected intravenously with $1 \cdot 10^7$ CatS deficient bone marrow derived cells obtained from CatS^{-/-} x LDLr^{-/-} mice that were generated as previously described.²⁹ Bone marrow from CatS^{+/+} x LDLr^{-/-} littermates was used as control. Mice were placed on a high-fat diet containing 0.25% cholesterol (Special Diets Services, Witham, Essex, UK) 5 weeks after transplantation. Both diet and water were provided ad libitum and continued for 12 weeks before euthanization. All animal work was approved by the regulatory authority of Leiden and performed in compliance with the Dutch government guidelines.

Genotyping and plasma cholesterol analysis

After euthanization, bone marrow was harvested for genotyping in order to verify that recipient bone marrow cells had been replaced by donor bone marrow. Bone marrow cells were obtained by flushing both femurs and tibiae with PBS. Double knockout genotypes were confirmed by PCR of genomic DNA as described.^{10, 30} After an overnight fasting-period, approximately 100 μ l blood was drawn from each individual mouse by tail bleeding every two weeks. Concentrations of total plasma cholesterol were determined by enzymatic procedures (Boehringer Mannheim, Germany). Precipath (standardized serum; Boehringer Mannheim, Germany) was used as an internal standard.

Tissue harvesting and preparation for histological analysis

Mice were euthanized 17 weeks after transplantation (at 12 weeks of diet). Before harvesting, the arterial bed was perfused with phosphate buffered saline (PBS) and 4% formaldehyde. Transverse, serial cryosections were prepared from OCT-embedded aortic roots (10 μ m thickness) and routinely stained with haematoxylin (Sigma Diagnostics) and eosin (Merck Diagnostica) and with Masson trichrome (Sigma). Five HE stained sections per mouse were selected for morphometry, digitized and analyzed as previously described.³¹

Corresponding sections were stained immunohistochemically with antibodies directed against mouse metallophilic macrophages (monoclonal mouse IgG_{2a}, clone MOMA2, dilution 1:50; Sigma Diagnostics, St. Louis, MO) and α -SM-actin (monoclonal IgG_{2a}, clone 1A4, dilution 1:100; Sigma). Macrophage, SMC and collagen positive areas were determined by computer-assisted color-gated measurement, and related to the total intimal surface area (Leica QWin). Lesions were classified according to average foam cell size: Type I lesions contain no or small foam cells, Type II reflects plaques that mostly enclose small, but also contain few large foam cells, while type III lesions are mostly constituted of large foam cells.³² The elastic lamina was visualized by autofluorescence on Oil Red O stained sections and lamina degradation was expressed as number of ruptures per mouse. To assess intimal cell death, sections were subjected to TUNEL staining according to protocols provided by the manufacturer (Roche Diagnostics). TUNEL positive cells, showing cell shrinkage, membrane blebbing or nuclear condensation³³, were counted and related to the total number of intimal cells.

Synthesis of CLIK60 and CatS activity assay

To inhibit CatS activity, the selective CatS inhibitor CLIK60 was prepared in-house according to the procedures described by Katunuma et al and had nuclear magnetic resonance, infrared and mass spectra consistent with the structure of the compound.³⁴ The purity of the compound used in this study was determined to be >97% by HPLC analysis. CLIK60 has been reported to inhibit 100% of CatS activity at 10^{-6} M and 86% at 10^{-7} M and shows virtually no inhibition of other cathepsins.³⁴ Cathepsin S activity was measured using the internally quenched fluorogenic peptide substrate Z-Phe-Val-Arg-AMC. Cell lysate samples were 10-fold diluted in CatS buffer (200 mM Na Acetate buffer pH 5.5, 4 mM EDTA, 8 mM DTT in 0.1% CHAPS). Conversion of the substrate was assessed in presence or absence of 10 μ M E64, a general cathepsin inhibitor, or various concentrations of CLIK60. The initial rate of substrate conversion (linear increase of fluorescence in time) was used as a measure of cathepsin S activity. AMC release was measured in real-time for 30 min at 28°C using a fluorescence plate reader (HTS 7000 BioAssay Reader; PerkinElmer Life and Analytical Sciences, Boston, MA).

Primary macrophage isolation

Peritoneal macrophages were isolated from male C57Bl/6 mice, as described previously.³⁵ Briefly, mice were injected intraperitoneally with 1 ml sterile Brewer's thioglycolate. On day 5, peritoneal cells were harvested, washed repeatedly (500 g for 10 min at 4°C), and resuspended in standard medium (Dulbecco's modified Eagle's medium (DMEM)) containing 20 mM HEPES, 4 mM glutamine, penicillin-streptomycin solution) with 10% FCS. Cells were seeded into 0.1% gelatin-coated 24-wells tissue-culture plates (5.0 $\cdot 10^5$ cells/well) and incubated at 37°C (5% CO₂) to allow cells to adhere. Non-adherent cells were removed by washing with PBS, and remaining cells were re-fed with standard medium.

Apoptosis and proliferation experiments

After an 8h pre-incubation with soluble elastin (1-10 ng/mL) +/- lactose (100 mM), an inhibitor of the elastin receptor ³⁶, or with CLIK60 (10⁻⁶ / 10⁻⁷ M), peritoneal macrophages and RAW 264.7 cells were incubated for 18h - in the presence of above mentioned vehicles - with 10 μM cisplatin or 25 μg/mL oxLDL to induce apoptosis. To assess cell death, cells were gently washed with PBS/1 mM EDTA, brought into suspension and washed once more in standard medium. Externalized phosphatidylserine was labeled (15 min at 0°C) with Annexin V (1 mg/mL; Santa Cruz) in AV buffer (10 mM HEPES, 145 mM NaCl, 5 mM KCl, 1.0 mM MgCl₂·6H₂O, 1.8 mM CaCl₂·2H₂O; pH 7.4). Propidium iodide (3.3 μM) in AV buffer was added 1 min before analysis by flow cytometry on a FACScalibur (Becton Dickinson, San Jose, CA). In addition, IFN-γ (400 U) stimulated peritoneal macrophages were incubated for 48 h with or without 10⁻⁶ M CLIK60 on gelatin (0.1%), collagen type I (0.1%) or fibronectin (0.1%) coated cover slips. Cells were visualized with Hoechst 33258 and Annexin V by fluorescence microscopy.

To examine the effect of CatS inhibition on proliferation, RAW 264.7 cells were cultured in 24-well dishes, synchronized by culturing in serum-free media overnight and in standard culture media for an additional day. Proliferation rate was quantified by adding 1 μCi ³H-thymidine per mL culture medium and measuring uptake over 5 h.

Expression analysis

Peritoneal macrophages were incubated with CLIK60 (10⁻⁶ M) for 18h and RNA was isolated using the TRIZOL method (Invitrogen, Netherlands) according to the manufacturer's instructions. Purified RNA was DNase treated (DNase I, 10U/μg total RNA) and reverse transcribed (RevertAid M-MuLV Reverse Transcriptase) according to the protocols provided by the manufacturer. Quantitative gene expression analysis was performed on an ABI PRISM 7700 machine (Applied Biosystems, Foster City, CA) using SYBR Green technology. Primers were designed for murine Bax, Bcl-2, XIAP, Flip, p53, SRA, SRBI, ABCA1, ABCG1 and HMGCoA using PrimerExpress 1.7 (Applied Biosystems) and validated for identical efficiencies (table 1). Target gene mRNA levels were expressed relative to that of the housekeeping gene (36b4) and calculated by subtracting the threshold cycle number (Ct) of the target gene from the Ct of 36b4 and raising two to the power of this difference.

Table 1: Primersets (5'-3')

| | | |
|---------|------------------------------|----------------------------|
| CatS | CTTGAAGGGCAGCTGAAGCTG | GTAGGAAGCGTCTGCCTCATA |
| HPRT | TTGCTCGAGATGTCATG | AGCAGGTCAGCAAAGAACTTATAG |
| 36b4 | GGACCCGAGAAGACCTCCTT | GCACATCACTCAGAATTTCAATGG |
| SRA-I | GGTGGTAGTGGAGCCCATGA | CCCGTATATCCCAGCGATCA |
| SRB-I | GGCTGCTGTTTGCTGCG | GCTGCTTGATGAGGGAGGG |
| ABCA1 | GGTTTGGAGATGGTTATACAATAGTTGT | TTCCCGGAAACGCAAGTC |
| ABCG1 | AGGTCTCAGCCTTCTAAAGTTCCTC | TCTCTCGAAGTGAATGAAATTTATCG |
| HMGCoAR | TCTGGCAGTCAGTGGAACTATT | CCTCGTCTTCGATCCAATTT |
| Bcl-2 | TGTTGAATGAGTCTGGGCTTT | TTTGACCCAGAAATCCACTCACA |
| XIAP | GAGTTCTGATAGGAATTTCCCAAATT | AACGACCCGTGCTTCATATTCT |
| Bax | CGTGGTTGCCCTCTTACTTT | TGATCAGCTCGGGCACTTTA |
| Flip | GCAACCCAGACTGCACAA | CGTCTCCTGCCTTGCTTCAG |
| P53 | AGCTTTGAGGTTCTGTTTGTG | TCCTTTTTGCGGAAATTTCTTC |

Cholesterol efflux

Peritoneal macrophages were stimulated with 400U IFN-γ and incubated with or without CLIK60 (10⁻⁶ / 10⁻⁷ M) throughout the experiment. After an 18 h incubation, cells were loaded with 3 mg/mL cholesterol and 1 mg/mL ³H-cholesterol (0.5 μCi/mL) in standard culture medium containing 10% fatty acid-free BSA during the next 24 h and equilibrated in cholesterol-free media for another 24 h. Cholesterol efflux was induced by addition of human HDL (50 μg/mL) or ApoA1 (5 μg/mL) or BSA as a control. Total amount of efflux was measured by LCS analysis of cell lysate and supernatant after 24 h.

Statistics

Differences in plaque size were statistically analyzed for significance using the Mann-Whitney U test. Other plaque parameters and constituents as well as differences in ΔCt were compared using the two-tailed Student's *t*-test. The incidence of elastic lamina rupture was compared using the Yate's corrected two-sided Fisher exact test.

Results

Bone marrow transplantation (BMT) was performed with freshly isolated bone marrow cells from CatS^{-/-} x LDLr^{-/-} mice or their CatS^{+/+} littermates 24 h after lethal irradiation. The animals recovered well from BMT and were put on a high-fat diet 5 weeks later. This resulted in a steady elevation of plasma cholesterol levels (850±150 mg/dL to 1980±190 mg/dL) and bodyweight over a period of twelve weeks during which both parameters did not differ between groups (data not shown).

To verify if bone marrow replacement was successful, CatS genotyping was performed on genomic DNA from bone marrow derived cells after euthanization 18 weeks post-BMT. This showed that CatS^{-/-} BMT resulted in an almost complete depletion of autologous bone marrow (data not shown). Immunostaining revealed that the intimal CatS content had been reduced by approximately 50% (P=0.004). In CatS^{-/-} transplanted animals CatS protein levels were preserved in SMC rich areas, such as the media and the fibrous cap (Figure 1A-C).

No effect on lesion size, but a dramatic change in plaque morphology

Advanced lesions developed after 12 weeks and did not display any differences in plaque size between groups (Figure 2A). Because the main focus of this study was the effect of leukocyte CatS deficiency on plaque stability, lesion morphology and composition in advanced lesions were carefully analyzed and revealed a marked change in plaque phenotype. Mice with CatS deficient leukocytes developed less progressed lesions compared to controls, although plaque size was the same. Only 36% of the plaques in the CatS^{-/-} BMT group showed a cap-core morphology compared to 82% in the control lesions (P=0.08) (Table 2). Instead, the majority of these lesions were phenotypically similar to large fatty streaks, containing a high amount of macrophage derived foam cells, with few SMCs and little collagen and lacking a necrotic core with an overlying fibrous cap (Figure 3A-D).

| Table 2: Distribution of plaque phenotypes | CatS ^{+/+} | CatS ^{-/-} | P-value |
|---|---------------------|---------------------|---------|
| Plaque Phenotype (AHA/ACC) | | | |
| Type II-III | 2 | 7 | |
| Type IV-VI | 9 | 4 | 0.08 |
| Foam Cell Size (Kawano, 2002; ref. 32) | | | |
| Type I | 6 | 0 | |
| Type II | 5 | 7 | |
| Type III | 0 | 4 | 0.006 |

Leukocyte CatS deficiency resulted in decreased SMC and collagen content

The observed changes in plaque morphology were confirmed by quantification of several plaque constituents. Intimal macrophage content was slightly increased in CatS^{-/-} BMT lesions (CatS^{-/-}-BMT: 48±3% vs. CatS^{+/+}-BMT: 41±3%, P=0.02), whereas SMC content was dramatically decreased by 62% (CatS^{-/-}-BMT: 3.7±1.6% vs. CatS^{+/+}-BMT: 9.7±2.1%, P=0.007) (Figure 2B-C). In discordance to SMC content, intimal collagen was reduced by only 33% from 17% in controls to 12% in the CatS^{-/-} BMT group (P=0.02) (Figure 2D). Surprisingly, the collagen : SMC ratio increased from 2.0±0.3 in controls to 6.2±0.8 in CatS^{-/-} BMT lesion (P=0.03), indicating that, in addition to reduced collagen synthesis as a consequence of decreased SMC numbers, collagen degradation was impaired as well in the absence of leukocyte CatS, resulting in a disproportional reduced collagen content.

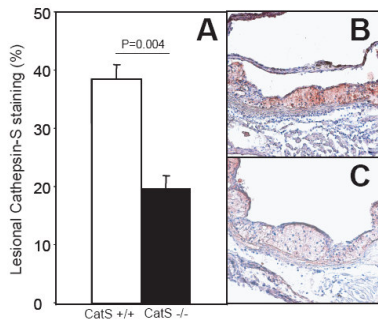


Figure 1. **A.** Transplantation of CatS deficient bone marrow to irradiated recipients resulted in a 50% reduction of CatS protein levels within the atherosclerotic lesions ($P=0.004$). **B.** Mice that received CatS+/+ bone marrow cells ubiquitously expressed CatS throughout the plaque, particularly in macrophage rich areas. **C.** CatS-/- BMT resulted in strongly reduced intimal CatS levels. CatS expression was preserved in SMC rich areas, such as the tunica media and the fibrous cap.

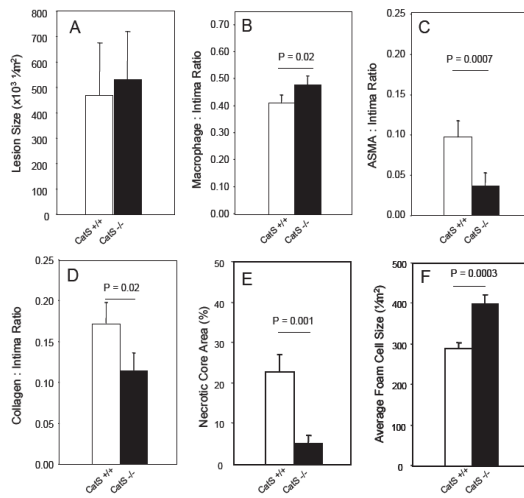


Figure 2. **A.** Total plaque size in the aortic root was not different between groups. **B.** Relative macrophage content was moderately increased with leukocyte CatS deficiency ($P=0.02$). **C.** Plaque content of α -SM-actin positive smooth muscle cells was found to be reduced by 62% with leukocyte CatS deficiency ($P=0.0007$). **D.** Deposition of intimal collagen, as measured in trichrome stained sections, was reduced by 33% in the CatS-/- group. ($P=0.02$) **E.** In line with the morphologic features of the lesion, necrotic core area was significantly reduced after CatS-/- BMT ($P=0.001$). **F.** Foam cell size was measured in a large number of cells representative of general foam cell size within the lesion. Similar to the observed increase of foam cell type III lesions with CatS deficiency, average foam cell size was significantly increased ($P=0.0003$). Values are mean \pm SEM.

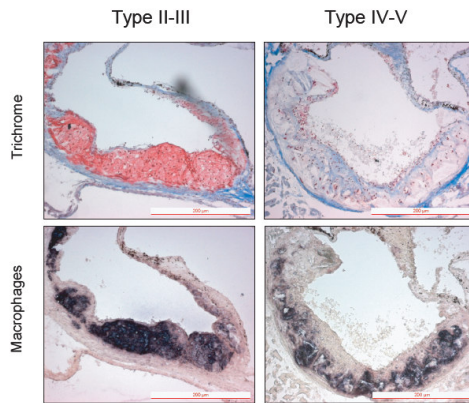


Figure 3. Two of the typical phenotypes that were observed stained with Masson trichrome and for macrophages (MoMa2). The distribution of each of these phenotypes is displayed in table 1. In the control group a advanced plaque cap-core morphology, corresponding with AHA type IV-VI lesions, could be observed in 82% of the plaques, while in the CatS-/- group 64% of the lesion showed a plaque morphology with no or only few small necrotic cores and large macrophage foam cells, analogous to AHA type II/III lesions.

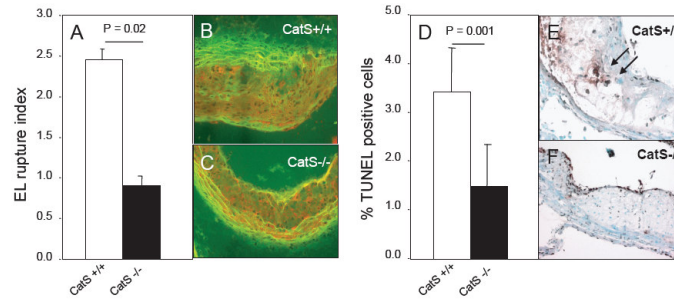


Figure 4. A-C. Impaired SMC content with leukocyte CatS could be explained by the 68% reduction of elastic lamina rupture after CatS^{-/-} BMT compared to controls (P=0.02). D-F. Decreased formation of necrotic cores with CatS deficiency could in part be explained by the 60% reduction of macrophage apoptosis as assessed with TUNEL staining (P=0.001). Values are mean ± SEM

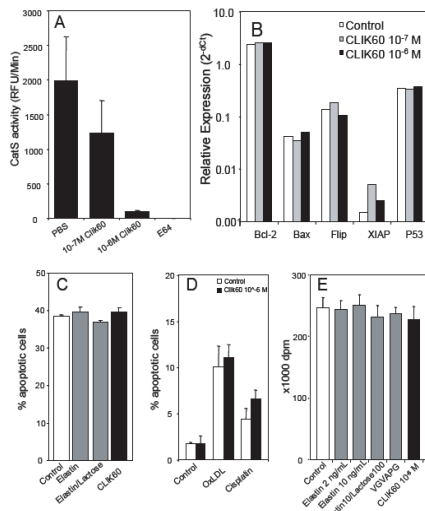


Figure 5. A. CatS activity in peritoneal macrophages from C57Bl/6 mice. Activity was dose-dependently reduced by the selective CatS inhibitor CLK60 and completely inhibited by the cysteine protease inhibitor E64. B. CLK60 did not directly affect expression of apoptosis related genes. C. Peritoneal macrophages were incubated with 25 μg/mL oxLDL to induce apoptotic cell death. CatS inhibition and soluble elastin fragments neither promoted, nor inhibited macrophage apoptosis as measured by flow cytometry on Annexin V/PI stained cells. D. Apoptosis was induced by 25 μg/mL oxLDL or 10 μM cisplatin in RAW cells. CLK60 did not result in an anti-apoptotic effect in these cells. E. Neither CatS inhibition nor soluble elastin fragments affected RAW cell proliferation rate measured by ³H-thymidine incorporation. Values are mean ± SEM.

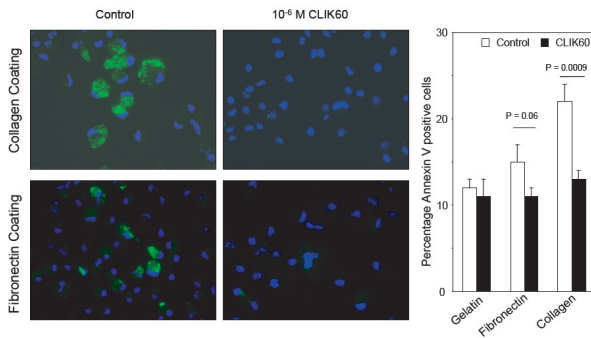


Figure 6. Peritoneal macrophages were plated on gelatin, fibronectin or collagen type I coated coverslips and stimulated with 400U IFN γ overnight to induce CatS expression. Apoptosis was assessed by staining externalized phosphatidylserine with Annexin V and increased in cells coated on fibronectin or collagen type I compared to cells coated on gelatin. This increase of apoptotic rate was prevented by selective CatS inhibition with CLK60. Values are mean ± SEM.

CatS deficiency reduced necrotic core area and increased foam cell size

Of the lesions in the CatS^{-/-} BMT group, 64% did not develop necrotic cores, while plaques that did, had smaller areas of necrosis. Necrotic core area was decreased by 77% from 22±4% in controls to only 5±2% in CatS^{-/-} BMT mice (Figure 2E). This reduction continued to exist even when excluding lesions that had not developed necrotic cores at all (data not shown). Furthermore, leukocyte CatS deficiency led to lesions that contained a higher amount of large macrophage foam cells (Type III), whereas control plaques enclosed mainly small and medium sized macrophages and macrophage derived foam cells (Type I&II lesions) (Table 1).³² This is reflected by a 38% increase of average foam cell size from 277±14 μm² in controls to 382±21 μm² in CatS^{-/-}BMT group (P=0.0003; Figure 2F).

Leukocyte CatS deficiency impaired elastolysis and attenuated apoptosis

SMC content depends on a variety of factors like proliferation, migration and PCM/ECM degradation. Upon stimulation SMCs will transmigrate to the intima through the elastic lamina. Degradation of the elastic lamina is vital for migration to take place and is mediated by the action of various proteases, such as MMP-8, CatK/S and to a lesser extent MMP-2 and -9. Indeed, leukocyte CatS deficiency led to a marked decrease by 68% of elastic lamina ruptures per mouse (CatS^{+/+}BMT: 2.45±0.13 ruptures/mouse vs. CatS^{-/-}BMT 0.91±0.11 ruptures/mouse), which suggests that leukocyte derived CatS is the predominant elastolytic enzyme in elastic lamina disruption (Figure 4A-C).

As intimal macrophage content and phenotype changed upon CatS deficiency and various studies have tentatively proposed a role for cathepsins in cell death^{7, 12}, lesions were TUNEL stained to assess apoptosis. Most commonly, TUNEL positive staining was found in foam cell rich or necrotic areas, principally indicating macrophage cell death. In accordance with the decreased necrotic core area, apoptotic rate was reduced by approximately 60% in lesions that contained CatS deficient leukocytes (P=0.001) (Figure 4D-F).

To study the effects of CatS deficiency in vitro, the selective CatS inhibitor CLIK60³⁷ was synthesized and validated for its inhibitory capacity. CatS activity in RAW 264.7 cells or peritoneal macrophages from C57Bl/6 or LDLr^{-/-} mice was completely repressed by CLIK60 at 10⁻⁶ M (Figure 5A). Apoptotic cell death was induced by 25 μg/mL Cu⁺⁺-oxidized LDL or 10 μM cisplatin. Inhibition of CatS activity did not affect RNA expression of the apoptosis related genes Bcl-2, Bax, P53 or Flip (Figure 5B). XIAP expression was increased by 70%, but this was not significant (P=0.16). Spontaneous or oxLDL/cisplatin induced apoptotic rate measured by flow cytometry analysis of AnnexinV/PI stained cells was not affected by CLIK60 treatment, pointing to a more indirect role for CatS in apoptosis (Figure 5C).

Matrix degradation products and apoptosis

To test the hypothesis that elastin degradation products, derived from CatS elastolytic activity, induced apoptosis, oxLDL treated peritoneal macrophages were incubated with 10 μg/mL soluble elastin with or without 100 mM lactose, an inhibitor of the laminin/elastin receptor. Elastin degradation products neither aggravated nor attenuated apoptotic or necrotic cell death of peritoneal macrophages (Figure 5D) nor did they affect macrophage proliferation (Figure 5E).

Alternatively, CatS could effect a disruption of cell-matrix interaction of macrophages in the surrounding PCM/ECM. To test this, peritoneal macrophages were cultured on gelatin, collagen type I or fibronectin coated dishes and stimulated with 400U IFN- γ , a powerful CatS inducer²⁰, and the effect of CLIK60 on apoptosis in this context was assessed by AnnexinV staining. Cells became progressively less viable when cultured on a fibronectin or collagen matrix compared to those that were cultured on gelatin. The amount of apoptotic cells, however, remained at the level of the gelatin cultured cells, when cells were treated with 10^{-6} M CLIK60 (Figure 6A-E), suggesting that CatS contributes to the increased apoptosis of fibronectin or collagen attached macrophages.

CatS inhibition dose-dependently increased macrophage cholesterol efflux

Because intracellular accumulation of free cholesterol has been reported to be an important inducer of apoptosis³⁸, the effect of CatS inhibition on the cholesterol efflux capacity of peritoneal macrophages was studied. CLIK60 led to a dose dependent increase of cholesterol efflux, enhancing HDL induced cholesterol efflux almost 2-fold ($P=0.001$) at a concentration of 10^{-6} M, indicating that CatS might contribute to apoptosis through retention of free cholesterol in the intracellular environment (Figure 7A). CatS inhibition did not affect genes involved in macrophage cholesterol metabolism (Figure 7B), indicating that CatS mediated modification of the extracellular cholesterol acceptor, i.e. HDL, causes the impaired cholesterol efflux.

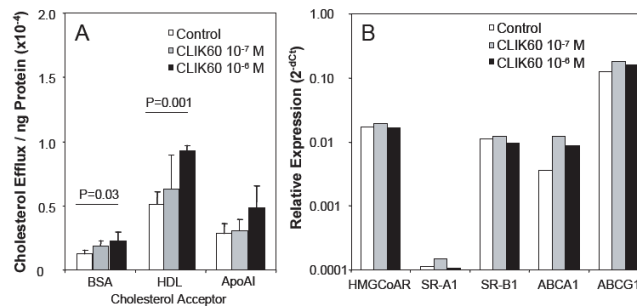


Figure 7. **A.** Cholesterol efflux from peritoneal macrophages preloaded with 3 H-cholesterol was induced by incubation with human HDL or apoAI. Both HDL and apoAI mediated cholesterol efflux was enhanced by CatS inhibition with CLIK60 in a dose-dependent manner. **B.** CLIK60 did not change expression of genes involved in macrophage lipid metabolism. Values are mean \pm SEM.

Discussion

Since Sukhova et al first described the presence of CatS in human atherosclerotic plaques²⁰, it has become increasingly clear that this protease is a key actor in atherogenesis and other related vasculopathies. Given its pleiotropic actions in inflammation, cell and matrix turnover and cholesterol trafficking it is important to carefully map the cell specific effects of this enzyme in atherosclerosis. This study is the first to establish the role of leukocyte CatS in atherosclerotic plaques. Cellular and matrix composition of advanced plaques was dramatically altered in mice that were transplanted with CatS deficient bone marrow, showing a 62% decrease of SMC content, which could, at least in part, be explained by a marked decrease in elastic lamina ruptures, pivotal for SMC migration into the intima. The disproportional reduction of intimal collagen by 33%, suggests that CatS is also directly involved in intimal collagen breakdown and turnover. Previous studies by Sukhova regarding CatS^{-/-} mice already showed impaired lamina degradation and reduced intimal SMC and collagen content.²⁶ The present study shows that macrophage, and not SMC, derived CatS is instrumental in the degradation of the inner elastic lamina.

Elastin degradation products have previously been reported to be able to promote SMC proliferation via the elastin/laminin receptor.³⁹ Conceivably, in this study absence of the elastolytic CatS might have contributed to impaired intimal SMC accumulation. However, no effect of degraded elastin could be detected on RAW264.7 cell proliferation, nor was there any effect of elastin degradation products on macrophage apoptosis, either spontaneous or induced with oxLDL or cisplatin.

Earlier studies demonstrated that systemic CatS deficiency impairs monocyte transmigration through an endothelial barrier.²⁶ By contrast, monocyte infiltration was not repressed and lesional macrophage staining area was even increased in the absence of leukocytic CatS. Possibly, staining of dead macrophages may have led to an underestimation of this difference. Thus, while earlier studies showed impaired monocyte transmigration through the endothelium in CatS^{-/-} mice²⁶, the present observations suggest that endothelial cell, and not monocyte, derived CatS is vital for leukocyte transmigration. The relative increase of intimal macrophages and the higher abundance of large foam cells in this study could be explained by the vast reduction in necrotic core formation and reduced susceptibility of macrophages to apoptosis in the absence of CatS.

Several studies show that lysosomal enzymes, including Cathepsin B, D and L, can directly induce apoptosis once released from the lysosomal compartment.^{12, 40-42} We now show that CatS inhibition by CLIK60 did not directly affect apoptosis or necrosis in macrophages that were stimulated with oxLDL or cisplatin. Moreover, the expression levels of several apoptosis related genes remained unaffected by CLIK60.

Secondly, impaired antigen presentation and impaired maturation of NKT cells might have affected viability of lesional macrophages.¹⁵ However, decreased NKT activity has been reported to markedly reduce plaque growth⁴³, while in the present study no effect on lesion size could be detected, implicating that NKT maturation only is a minor factor in this regard.

Additionally, degradation of ECM constituents, disturbing cell-cell and cell-matrix interactions, has been reported to be an important mediator of cell death.^{7, 42, 44, 45} As mentioned earlier, soluble elastin degradation products did not affect both apoptosis and proliferation of macrophages *in vitro*. Interestingly, macrophages cultured on fibronectin or collagen type I showed an increased apoptotic rate compared to macrophages that were cultured on gelatin. Inhibition of CatS activity prevented this induction of apoptosis and kept the rate of cell death to the baseline level of gelatin

cultured macrophages. These observations suggest that CatS induces apoptosis by mediating pericellular fibronectin and collagen type I breakdown and thus is an important regulator of macrophage apoptosis *in vivo*.

Finally, free cholesterol is a potent inducer of apoptosis in macrophages by triggering cytochrome c release and activating FasL.^{38, 46, 47} In line with earlier observations regarding the inhibitory action of CatS on cholesterol efflux¹⁷, CatS inhibition was found to potentiate both HDL and apoA1 induced cholesterol efflux from peritoneal macrophages. It is feasible that impaired efflux of intracellular accumulated cholesterol from foam cells by CatS importantly contributes to programmed cell death in atherosclerotic lesions and thus to necrotic core formation. Figure 8 summarizes the proposed pathways of macrophage derived CatS in the vascular wall with regard to collagen deposition and apoptosis.

In conclusion, we show that leukocytic CatS is a key modulator in the pathobiology of atherosclerosis. Medial SMC migration into the intima and subsequent proliferation and collagen deposition notably relies on the elastolytic properties of macrophage derived CatS. Moreover, the present data show that macrophage viability is threatened by CatS through several mechanisms, among which disruption of cell-matrix interactions and impaired efflux of free cholesterol, resulting in CatS mediated apoptotic cell death. Although the exact role of CatS from other cellular sources and their interplay with leukocytic CatS remains to be elucidated, the imperative contribution of macrophage CatS to the expansion of necrotic cores in advanced plaques implies that it is likely involved in plaque destabilization, which might eventually lead to acute ischemic events.

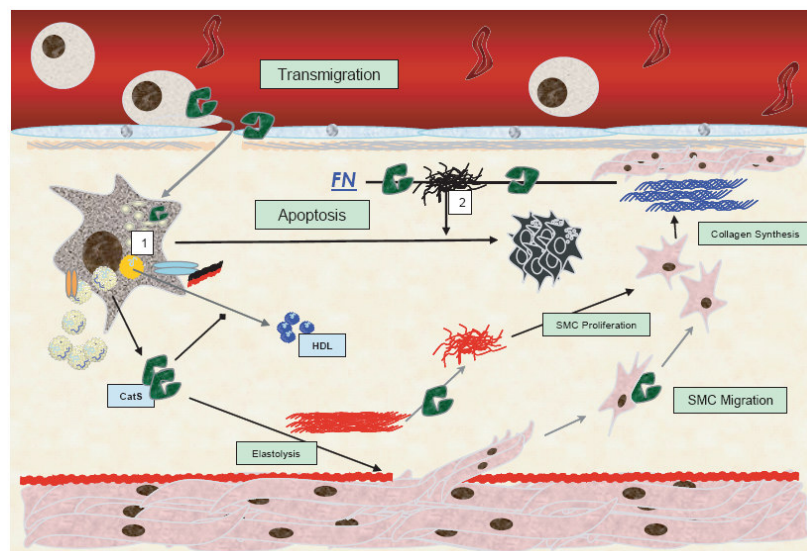


Figure 8. Possible mechanisms that contributed to the observed decrease in SMC and collagen content and macrophage apoptosis upon leukocyte CatS deficiency. The number of elastic lamina ruptures was markedly reduced after CatS^{-/-} BMT, suggesting that macrophage derived CatS is an important contributor to degradation of the elastic lamina and can be a limiting factor in SMC migration into the intima and thus collagen deposition. In addition, degradation products from intimal elastin have a proliferative effect on SMCs *in vitro* (39) and in this way CatS may also influence intimal SMC content. CatS can promote macrophage apoptosis through 1) inhibiting efflux of pro-apoptotic free cholesterol by modifying HDL in the intima and 2) degradation of fibronectin (FN) and collagen type I, hence disrupting cell-matrix interaction to favor cell survival.

References

1. Katsuda S, Kaji T. Atherosclerosis and extracellular matrix. *J Atheroscler Thromb.* 2003;10(5):267-274.
2. Bergers G, Brekken R, McMahon G, et al. Matrix metalloproteinase-9 triggers the angiogenic switch during carcinogenesis. *Nat Cell Biol.* Oct 2000;2(10):737-744.
3. Garcia-Touchard A, Henry TD, Sangiorgi G, et al. Extracellular Proteases in Atherosclerosis and Restenosis. *Arterioscler Thromb Vasc Biol.* Jun 2005;25(6):1119-1127.
4. Lutun A, Carmeliet P. Genetic studies on the role of proteinases and growth factors in atherosclerosis and aneurysm formation. *Ann N Y Acad Sci.* Dec 2001;947:124-132; discussion 132-123.
5. Freestone T, Turner RJ, Coady A, et al. Inflammation and matrix metalloproteinases in the enlarging abdominal aortic aneurysm. *Arterioscler Thromb Vasc Biol.* Aug 1995;15(8):1145-1151.
6. Newby AC. Dual role of matrix metalloproteinases (matrixins) in intimal thickening and atherosclerotic plaque rupture. *Physiol Rev.* Jan 2005;85(1):1-31.
7. Lindstedt KA, Leskinen MJ, Kovanen PT. Proteolysis of the pericellular matrix: a novel element determining cell survival and death in the pathogenesis of plaque erosion and rupture. *Arterioscler Thromb Vasc Biol.* Aug 2004;24(8):1350-1358.
8. Belotti D, Paganoni P, Manenti L, et al. Matrix metalloproteinases (MMP9 and MMP2) induce the release of vascular endothelial growth factor (VEGF) by ovarian carcinoma cells: implications for ascites formation. *Cancer Res.* Sep 1 2003;63(17):5224-5229.
9. Riese RJ, Mitchell RN, Villadangos JA, et al. Cathepsin S activity regulates antigen presentation and immunity. *J Clin Invest.* Jun 1 1998;101(11):2351-2363.
10. Shi GP, Villadangos JA, Dranoff G, et al. Cathepsin S required for normal MHC class II peptide loading and germinal center development. *Immunity.* Feb 1999;10(2):197-206.
11. Shi GP, Bryant RA, Riese R, et al. Role for cathepsin F in invariant chain processing and major histocompatibility complex class II peptide loading by macrophages. *J Exp Med.* Apr 3 2000;191(7):1177-1186.
12. Li W, Yuan XM. Increased expression and translocation of lysosomal cathepsins contribute to macrophage apoptosis in atherogenesis. *Ann N Y Acad Sci.* Dec 2004;1030:427-433.
13. Hentze H, Lin XY, Choi MS, et al. Critical role for cathepsin B in mediating caspase-1-dependent interleukin-18 maturation and caspase-1-independent necrosis triggered by the microbial toxin nigericin. *Cell Death Differ.* Sep 2003;10(9):956-968.
14. Liu W, Spero DM. Cysteine protease cathepsin S as a key step in antigen presentation. *Drug News Perspect.* Jul-Aug 2004;17(6):357-363.
15. Riese RJ, Shi GP, Villadangos J, et al. Regulation of CD1 function and NK1.1(+) T cell selection and maturation by cathepsin S. *Immunity.* Dec 2001;15(6):909-919.
16. Driessen C, Bryant RA, Lennon-Dumenil AM, et al. Cathepsin S controls the trafficking and maturation of MHC class II molecules in dendritic cells. *J Cell Biol.* Nov 15 1999;147(4):775-790.
17. Lindstedt L, Lee M, Oorni K, et al. Cathepsins F and S block HDL3-induced cholesterol efflux from macrophage foam cells. *Biochem Biophys Res Commun.* Dec 26 2003;312(4):1019-1024.
18. Hakala JK, Oksjoki R, Laine P, et al. Lysosomal enzymes are released from cultured human macrophages, hydrolyze LDL in vitro, and are present extracellularly in human atherosclerotic lesions. *Arterioscler Thromb Vasc Biol.* Aug 1 2003;23(8):1430-1436.
19. Camejo G. Hydrolytic enzymes released from resident macrophages and located in the intima extracellular matrix as agents that modify retained apolipoprotein B lipoproteins. *Arterioscler Thromb Vasc Biol.* Aug 1 2003;23(8):1312-1313.
20. Sukhova GK, Shi GP, Simon DI, et al. Expression of the elastolytic cathepsins S and K in human atheroma and regulation of their production in smooth muscle cells. *J Clin Invest.* Aug 1 1998;102(3):576-583.
21. Whitman SC, Ravisankar P, Elam H, et al. Exogenous interferon-gamma enhances atherosclerosis in apolipoprotein E-/- mice. *Am J Pathol.* Dec 2000;157(6):1819-1824.
22. Tellides G, Tereb DA, Kirkiles-Smith NC, et al. Interferon-gamma elicits arteriosclerosis in the absence of leukocytes. *Nature.* Jan 13 2000;403(6766):207-211.
23. Storm van's Gravesande K, Layne MD, Ye Q, et al. IFN regulatory factor-1 regulates IFN-gamma-dependent cathepsin S expression. *J Immunol.* May 1 2002;168(9):4488-4494.
24. Cheng XW, Kuzuya M, Sasaki T, et al. Increased expression of elastolytic cysteine proteases, cathepsins S and K, in the neointima of balloon-injured rat carotid arteries. *Am J Pathol.* Jan 2004;164(1):243-251.
25. Jormsjo S, Wuttge DM, Sirsjo A, et al. Differential expression of cysteine and aspartic proteases during progression of atherosclerosis in apolipoprotein E-deficient mice. *Am J Pathol.* Sep 2002;161(3):939-945.
26. Sukhova GK, Zhang Y, Pan JH, et al. Deficiency of cathepsin S reduces atherosclerosis in LDL receptor-deficient mice. *J Clin Invest.* Mar 2003;111(6):897-906.

27. Shi GP, Sukhova GK, Kuzuya M, et al. Deficiency of the cysteine protease cathepsin S impairs microvessel growth. *Circ Res*. Mar 21 2003;92(5):493-500.
28. Celletti FL, Waugh JM, Amabile PG, et al. Vascular endothelial growth factor enhances atherosclerotic plaque progression. *Nat Med*. Apr 2001;7(4):425-429.
29. van Eck M, Bos IS, Kaminski WE, et al. Leukocyte ABCA1 controls susceptibility to atherosclerosis and macrophage recruitment into tissues. *Proc Natl Acad Sci U S A*. Apr 30 2002;99(9):6298-6303.
30. Ishibashi S, Brown MS, Goldstein JL, et al. Hypercholesterolemia in low density lipoprotein receptor knockout mice and its reversal by adenovirus-mediated gene delivery. *J Clin Invest*. Aug 1993;92(2):883-893.
31. von der Thusen JH, van Vlijmen BJ, Hoeben RC, et al. Induction of atherosclerotic plaque rupture in apolipoprotein E-/- mice after adenovirus-mediated transfer of p53. *Circulation*. Apr 30 2002;105(17):2064-2070.
32. Kawano H, Yano T, Mizuguchi K, et al. Changes in aspects such as the collagenous fiber density and foam cell size of atherosclerotic lesions composed of foam cells, smooth muscle cells and fibrous components in rabbits caused by all-cis-5, 8, 11, 14, 17-icosapentaenoic acid. *J Atheroscler Thromb*. 2002;9(4):170-177.
33. Kockx MM. Apoptosis in the atherosclerotic plaque: quantitative and qualitative aspects. *Arterioscler Thromb Vasc Biol*. Oct 1998;18(10):1519-1522.
34. Katunuma N, Tsuge H, Nukatsuka M, et al. Structure-based design of specific cathepsin inhibitors and their application to protection of bone metastases of cancer cells. *Arch Biochem Biophys*. Jan 15 2002;397(2):305-311.
35. Herijgers N, Van Eck M, Groot PH, et al. Low density lipoprotein receptor of macrophages facilitates atherosclerotic lesion formation in C57Bl/6 mice. *Arterioscler Thromb Vasc Biol*. Aug 2000;20(8):1961-1967.
36. Faury G, Usson Y, Robert-Nicoud M, et al. Nuclear and cytoplasmic free calcium level changes induced by elastin peptides in human endothelial cells. *Proc Natl Acad Sci U S A*. Mar 17 1998;95(6):2967-2972.
37. Katunuma N, Murata E, Kakegawa H, et al. Structure based development of novel specific inhibitors for cathepsin L and cathepsin S in vitro and in vivo. *FEBS Lett*. Sep 10 1999;458(1):6-10.
38. Tabas I. Apoptosis and plaque destabilization in atherosclerosis: the role of macrophage apoptosis induced by cholesterol. *Cell Death Differ*. Jul 2004;11 Suppl 1:S12-16.
39. Mochizuki S, Brassart B, Hinek A. Signaling pathways transduced through the elastin receptor facilitate proliferation of arterial smooth muscle cells. *J Biol Chem*. Nov 22 2002;277(47):44854-44863.
40. Li W, Yuan XM, Olsson AG, et al. Uptake of oxidized LDL by macrophages results in partial lysosomal enzyme inactivation and relocation. *Arterioscler Thromb Vasc Biol*. Feb 1998;18(2):177-184.
41. Li W, Dalen H, Eaton JW, et al. Apoptotic death of inflammatory cells in human atheroma. *Arterioscler Thromb Vasc Biol*. Jul 2001;21(7):1124-1130.
42. Michel JB. Anoikis in the cardiovascular system: known and unknown extracellular mediators. *Arterioscler Thromb Vasc Biol*. Dec 2003;23(12):2146-2154.
43. Nakai Y, Iwabuchi K, Fujii S, et al. Natural killer T cells accelerate atherogenesis in mice. *Blood*. Oct 1 2004;104(7):2051-2059.
44. Meilhac O, Ho-Tin-Noe B, Houard X, et al. Pericellular plasmin induces smooth muscle cell anoikis. *Faseb J*. Jul 2003;17(10):1301-1303.
45. Laouar A, Glesne D, Huberman E. Protein kinase C-beta, fibronectin, alpha(5)beta(1)-integrin, and tumor necrosis factor-alpha are required for phorbol diester-induced apoptosis in human myeloid leukemia cells. *Mol Carcinog*. Dec 2001;32(4):195-205.
46. Yao PM, Tabas I. Free cholesterol loading of macrophages is associated with widespread mitochondrial dysfunction and activation of the mitochondrial apoptosis pathway. *J Biol Chem*. Nov 9 2001;276(45):42468-42476.
47. Yao PM, Tabas I. Free cholesterol loading of macrophages induces apoptosis involving the fas pathway. *J Biol Chem*. Aug 4 2000;275(31):23807-23813.

